Interferometric alignment and figure testing of large (0.5 m) off-axis parabolic mirrors in a challenging cleanroom environment

Robert H. Barkhouser[*a], Raymond G. Ohl[†a,b]

[a]Department of Physics and Astronomy, The Johns Hopkins University

[b]Astronomy Department, University of Virginia

ABSTRACT

The Far Ultraviolet Spectroscopic Explorer (FUSE), successfully launched in June 1999, is an astrophysics satellite designed to provide high resolution spectra ($\lambda/\Delta\lambda$ = 24,000-30,000) with large effective area (20-70 cm^2) over the interval 90.5-118.7 nm. The FUSE instrument consists of four co-aligned, off-axis parabolic primary mirrors which focus light into separate spectrograph channels. The mirrors are rectangular (407 × 372 mm) and fabricated from lightweighted Zerodur blanks.

We describe a straightforward method for aligning these off-axis parabolas in an autocollimation setup via qualitative and quantitative analysis of static interferograms. Initial alignment is achieved rapidly by visual inspection of the interferogram as adjustments are made in vertical and horizontal alignment. Fine alignment to the limit of the optical system then proceeds with small alignment steps and fringe analysis software to find the position which minimizes wavefront error. This method was used for figure testing the FUSE primary mirrors throughout build-up and qualification of the flight mirror assemblies.

The far-ultraviolet reflectivity of the FUSE mirrors is very sensitive to molecular contamination. All mirror testing thus took place in a strictly controlled class 1000 cleanroom environment. In addition to the challenging vibration and turbulence problems this environment presented, two of the flight mirrors were coated with lithium fluoride over aluminum. This necessitated purging the setup with dry nitrogen, as the lithium fluoride coating degrades with exposure to water vapor. We discuss the difficulties these environmental constraints presented and summarize the mitigating action.

Keywords: FUSE, optical testing, alignment, interferometry, off-axis parabola, OAP

1. INTRODUCTION

The Far Ultraviolet Spectroscopic Explorer (FUSE), which began its three year mission on June 24, 1999, is a NASA astrophysics satellite that will obtain high resolution ($\lambda/\Delta\lambda$ = 24,000-30,000) spectra over the wavelength interval 90.5-118.7 nm. The instrument uses four co-aligned, off-axis parabolic (OAP) primary mirrors to collect and focus light for separate Rowland circle spectrograph channels (Figure 1). The spectrograph employs spherical, holographically ruled gratings and microchannel plate detectors with delay line anodes.[1] Each of the two detectors record spectra from a pair of instrument channels. In addition to these far-ultraviolet channels, two primary mirrors additionally provide visible light images for the Fine Error Sensors. Total instrument weight is approximately 730 kg.

The primary mirror assemblies[2] were integrated and tested in a cleanroom at The Johns Hopkins University (JHU).[3] A tight imaging requirement on the fully assembled flight mirrors required figure testing at several stages in the build-up procedure to monitor for assembly-induced distortion. This required an easily reconfigured metrology mount capable of supporting a mirror alone or with flight hardware attached. The tight schedule dictated a fast turn-around time for each test. The setup used for figure testing also had to support image testing in the ultraviolet (UV).[4] Very strict particulate contamination

[*] Correspondence: rhb@pha.jhu.edu; www.pha.jhu.edu/facilities/idg/; Telephone: 410 516 7918; Fax: 410 516 8260
[†] Correspondence: ohl@pha.jhu.edu; http://fuse.pha.jhu.edu; Telephone: 410 516 4375; Fax: 410 516 5494

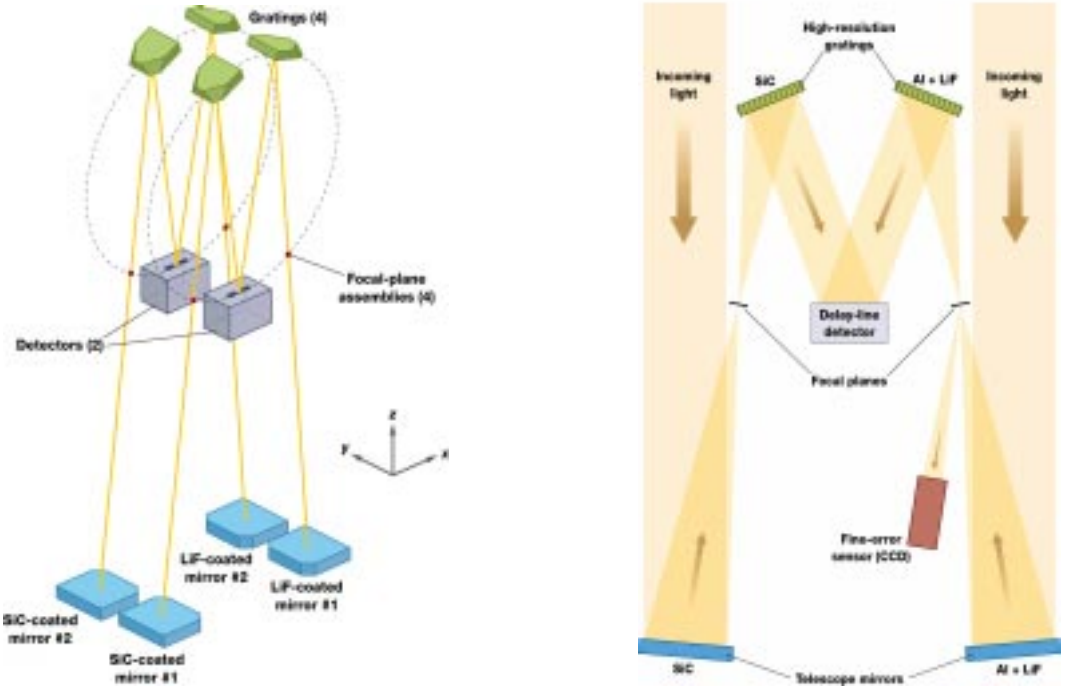

(a) (b)

Figure 1. (a) Schematic diagram of the FUSE optical design, showing four UV channels with each SiC/LiF pair sharing a single microchannel plate detector. (b) Light path sketch for half of the FUSE instrument (one SiC/LiF pair of UV channels). Also represented is one of two visible-light Fine Error Sensors.

levels for the flight optics required that the mirrors and assembly hardware be maintained in class 1000 cleanroom conditions at all times. The far-UV reflectivity of the optical coatings is extremely sensitive to molecular contamination, imposing additional requirements particularly in the areas of test and flight hardware material selection, preparation and handling. Two of the mirrors were coated with lithium fluoride (LiF) over aluminum, the far-UV reflectivity of which degrades rapidly with exposure to typical laboratory humidity levels.[5] Thus, all assembly and test fixturing had to accommodate a nitrogen (N_2) purge to maintain the optical surface under dry conditions. Finally, strict cost control and a "good enough" test philosophy drove many decisions concerning the hardware and instrumentation used for figure testing the mirrors.

We present a straightforward and detailed method for the interferometric alignment and figure testing of large-aperture OAP mirrors. We describe this method as applied to the primary mirrors on the FUSE instrument. We discuss how we addressed the issues listed above toward the successful completion of our test program. We also briefly discuss our procedure in comparison with other alignment methods.

2. MIRROR DESIGN, ASSEMBLY, AND TEST PLAN

2.1. Optical and Mechanical Design

The FUSE OAP mirrors are rectangular, having a 387 × 352 mm clear aperture, 2245 mm focal length, and 5.5° off-axis angle (Figure 2a). The substrates are Zerodur, 407 × 372 mm in size, and are 70% lightweighted with an open-back, triangular isogrid rib pattern (Figure 2b). This results in an average 7.5 mm facesheet thickness (the pockets have flat bottoms) and a final weight of about 17 lb. SVG Tinsley Laboratories* ("Tinsley") lightweighted and polished the mirror blanks. The mirrors are physically identical and polished to the same prescription in order to be interchangeable on the instrument optical bench. However, the actual off-axis sections are slightly different to optimize grating incidence angles

* Silicon Valley Group, Inc., Tinsley Division, Tinsley Laboratories, Richmond, CA

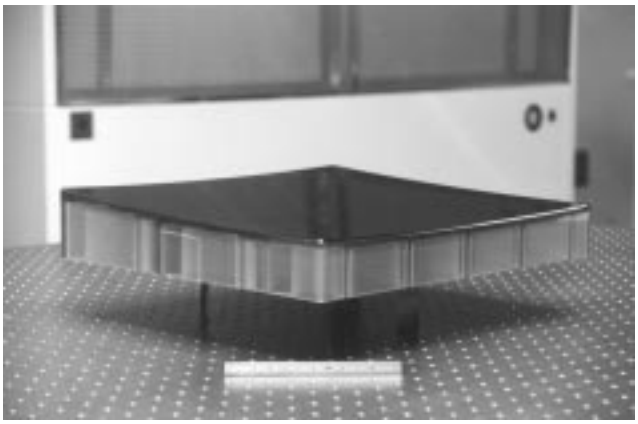

Raymond G. Ohl

(a)

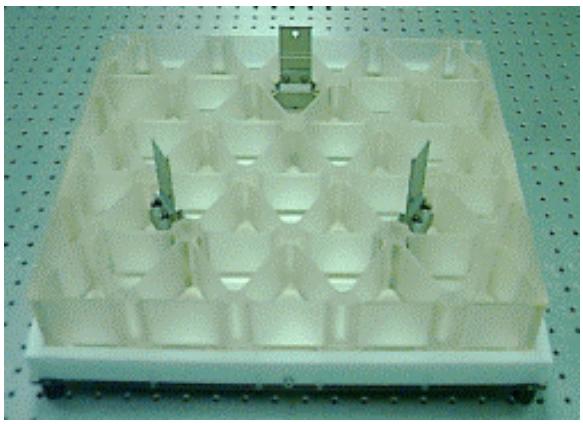

Raymond G. Ohl

(b)

Swales & Associates, Inc.

(c)

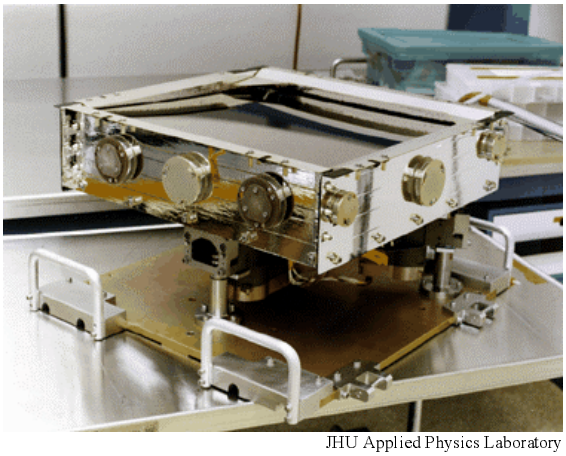

JHU Applied Physics Laboratory

(d)

Figure 2. (a) FUSE mirror resting face up on its flexures. (b) FUSE mirror face down in a protective purge enclosure. The open-back triangular rib pattern and three radial blade flexures are evident. (c) Mirror assembly showing aluminum dummy "mirror," composite intermediate plate, and tip/tilt/focus actuator assembly; mounted to a handling fixture. (d) Full flight mirror assembly with "pie pan" enclosure and aperture stop installed (polycarbonate purge/protective cover removed for photo); mounted to a handling fixture. Metrology mount hanger pins can be seen on right front edge of fixture. Smaller access ports on right front side of pie pan are identical to ones used for offloading mirror from assembly during figure testing.

for the different channel bandpasses, and the clear apertures are defined by an aperture stop located near each optical surface (Figure 2d). In addition to supplying some redundancy, the four independent optical channels allowed us to tailor the mirror coatings to maximize reflectivity in the FUSE bandpass. Two mirrors are coated with ion beam sputtered silicon carbide (SiC) and two are coated with lithium fluoride (LiF) over aluminum, to maximize reflectivity from 90.5-110.3 nm and 98.0-118.7 nm, respectively.[*]

The FUSE mirror assemblies have been described in detail elsewhere.[2] Each mirror is mounted to a composite "intermediate plate" via three radial blade flexures. The titanium flexure blades are attached to Invar fittings bonded to special mirror ribs. The intermediate plate consists of an aluminum honeycomb core sandwiched between graphite/cyanate ester facesheets, and is approximately 19 mm thick. Bonded-in fittings provide attachment surfaces for the mirror blade flexures. Below the intermediate plate, three precision ball screw actuators with sub-micron resolution allow tip/tilt and focus adjustment for each mirror, with enough range to compensate for expected pre-flight misalignment, gravity release in the instrument structure upon orbital insertion, and long-term shrinkage of the structure due to moisture desorption. The intermediate plate is attached to the actuator assembly via three post flexures coaxial with the ball screws; in addition, three

[*] The Optical Thin Film Laboratory at NASA/Goddard Space Flight Center (GSFC) coated the FUSE mirrors.

lateral post flexures secure the intermediate plate "in plane" (perpendicular to the optical axis). The primary function of the intermediate plate is to isolate the mirror from moments that can be induced by movement of the actuators.

To insure that adequate far-UV flux is transmitted through the high-resolution spectrograph slit (1.25 × 20 arcsec), the fully assembled flight mirrors had to meet the following encircled energy (EE) requirement: At a wavelength of 100 nm, 90% of the collected flux from a point source must be focused within a diameter of 1.5 arcsec, which corresponds to 16 μm at the focal plane. In order to meet this requirement, we established optical surface tolerances based on SOHO SUMER* mirror heritage.[6] We validated these tolerances with a modulation transfer function analysis carried out at JHU, and an independent study.[7] In addition to stringent midfrequency (≤ 20 Å RMS from 0.1-10 mm spatial periods) and microroughness (≤ 10 Å RMS) specifications, we required a figure error no worse than λ/40 RMS (λ = 632.8 nm). The figure error specification was later relaxed to λ/20 RMS in light of unavoidable assembly-induced distortions and schedule and budget constraints.[3] This relaxed specification broadened the image core, but had little effect on achieving the EE specification.[4]

2.2. Assembly Procedure

The first step in the build-up of the flight mirror assemblies was the bonding of the flexures to the mirror substrate. This took place before aspherizing the optical surface, due to unexpected effects from the epoxy we selected, which were discovered with an engineering test mirror.[3] Coating of the optical surface occurred immediately after each mirror was delivered to JHU. Once coated, the optical surface was maintained in a N_2 environment almost continually to preserve the far-UV reflectivity. Next, the mirror was mounted to the intermediate plate. This was the most sensitive and difficult portion of the assembly procedure, often requiring several attempts, because any moments inadvertently applied to the strong axis of the flexures would result in distortion of the optical surface. After figure testing verified acceptable surface error, the sub-assembly was subjected to a thermal-vacuum test to verify the mirror figure would not be significantly degraded by the vacuum and thermal conditions in space. The mirror flexures were then match drilled to the intermediate plate inserts and shear pins installed to prevent any movement at that interface.

At this point, the mirror and intermediate plate sub-assembly was mounted to the fully assembled actuator assembly, using three axial and three lateral post flexures. A thin-walled composite "pie pan" (Figure 2d) was then attached to the intermediate plate. The pie pan surrounds the mirror and minimizes heat transfer from the edges of the mirror substrate, as well as providing an enclosed purge volume when the (non-flight) protective polycarbonate mirror cover is installed. Lastly, the aperture stop is attached to the rim of the pie pan. Once fully assembled, the unit underwent vibration testing to simulate launch loads with sinusoid and random motions in three orthogonal axes.

2.3. Optical Figure Test Plan

Interferometric figure testing of each mirror surface was performed throughout the assembly build-up, culminating in a final figure test of the complete and flight-qualified unit. Other optical testing and analysis was carried out to assess the far-UV imaging performance of the mirrors,[4] but we concentrate here on the details of the surface figure testing.

In order to monitor the mirrors for assembly-induced distortion, we tested at the following stages of the build process:

1. after deposition of the reflective coatings (this established the baseline optical figure)
2. after attachment of the mirror to the intermediate plate (and any repeated attempts)
3. after thermal-vacuum testing
4. after drilling and pinning of the mirror flexures
5. full assembly, prior to vibration test
6. after vibration test (final figure test).

With four flight mirrors and one spare, a minimum of thirty OAP figure tests is indicated. In the end, the spare mirror was only carried through step 2, and a very few of the intermediate figure tests were skipped after we gained enough confidence in our hardware and procedures. Even so, the final tally was close to thirty because of the number of repeated attempts at

* Solar Ultraviolet Measurements of Emitted Radiation experiment on the Solar Heliospheric Observatory.

mounting a mirror to its intermediate plate with acceptable amounts of induced figure error. A spherical engineering mirror, used to qualify each step in the assembly and environmental test procedure, was figure-tested close to a hundred times in the course of developing our test method, optimizing the metrology mount, and working through assembly procedure problems. Fortunately, the spherical surface made alignment trivial in this case.

3. ALIGNMENT AND FIGURE TESTING

3.1. Test Setup and Method

In order to use an existing cleanroom at JHU, we tested the mirrors in an optical axis-horizontal setup. In addition, we required that the mirror be oriented such that the parabola vertex was to one side of the mirror, not above or below it. This kept the fixturing simple and the number of auxiliary optics to a minimum, a critical factor for the UV image testing which was to make use of the same basic setup. A finite-element model of the FUSE mirrors had been developed in the early design phase, and refined and validated during fabrication of the engineering mirror.[2] We used this model to verify that an axis-horizontal, vertex-to-the-side configuration was viable, without need of a complex G-negating metrology mount.

3.1.1. Metrology mount

One complication in the design of our metrology mount was the requirement to test the mirror at three stages of assembly: the mirror alone (with flexures attached), the mirror mounted to an intermediate plate, and the full mirror assembly including actuators and pie pan. Because the mirrors were assembled in parallel in a pipeline fashion, we had to be able to quickly reconfigure the metrology mount to handle any of the three mirror configurations. Figure 3 shows these configurations schematically and the methods used to support the mirror and offload the attached hardware.

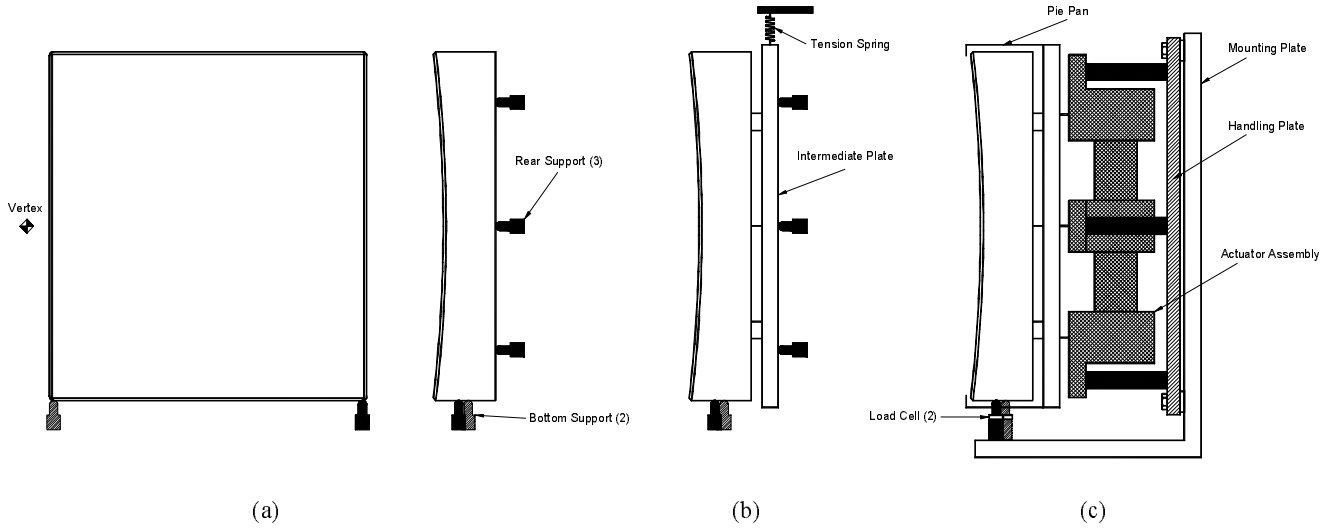

Figure 3. Schematic diagram of the three mirror support configurations. (a) Mirror only (blade flexures not shown here), shown face-on and from the anti-vertex side. The mirror is supported by two ball supports (one shown hashed, the other solid black) on the bottom edge just inboard from the corner radii, and leans backward very slightly against three rear supports (black) located at rib intersections in a triangular pattern. (b) Mirror and intermediate plate, shown from the anti-vertex side, with tension spring to offload the weight of the intermediate plate from the mirror flexures. (c) Full assembly, with handling plate bolted to metrology mount. Calibrated load cells are use to set proper force on bottom support points.

For the mirror alone (Figure 3a), two ball support points on the bottom edge of the substrate were used, one at each end just inside the radius at the corner. The support locations were optimized with a CAD solid model of the mirror, so that no twisting moments are introduced into the glass; this is why the vertex-side support (where the mirror is thinner) is closer to the back surface than the anti-vertex-side support (where the mirror is thicker). Using the locations specified by the model,

we found the mirror to be well balanced on the two support locations; we then moved the supports slightly forward so the mirror leaned back very lightly against three rear locating balls (referred to as "rear supports").

With the intermediate plate attached to the mirror, the same two bottom support locations were used. This was done by adjusting the rear supports backward by an amount equal to the distance from the back of the mirror to the back of the intermediate plate. With the intermediate plate then resting against the rear supports, the mirror itself was in the same position on the metrology mount as before when no intermediate plate was present. To offload the weight of the intermediate plate from the mirror flexures, a single tension spring was used at the neutral axis of the plate. The spring was calibrated by hanging an intermediate plate from it and measuring the distance between the spring hooks.

The full mirror assemblies were stored and transported on handling plates (Figures 2c and d), and the metrology mount was designed to interface to these plates. Basically, the handling plate was secured with bolts to three raised pads on the metrology mount vertical plate that had been lapped flat with respect to each other. The metrology mount plate was fitted with two hooks on its top edge; these engaged hanger pins (Figure 2d) on the handling plate to allow the assembly to be suspended in the proper position (without relying on muscle power) while the bolts were secured. At this point, the bottom mirror supports were raised up through access ports in the pie pan until contacting the mirror, in the same locations as had been used in the previous two configurations. These supports were equipped with load cells that had been calibrated in place with a bare mirror (no attached hardware other than mirror flexures). The supports were raised until the readings obtained during calibration were reported by the load cells.

3.1.2. Optical test setup

The double-pass optical layout is shown in Figure 4. In addition to its simplicity, the two reflections of the test beam off the OAP mirror made the setup more sensitive to distortions in the mirror surface. The optical hardware we employed for this testing consisted of the following:

1. laser unequal path interferometer (LUPI)[8] with f/4 diverger lens and CCD video camera[*]
2. 2" square Zerodur fold flat, $\lambda/20$ surface flatness at 632.8 nm[†]
3. 21" diameter ULE autocollimating (AC) flat, $\lambda/20$ surface flatness at 632.8 nm, sub-arcsecond tip/tilt mount[‡]
4. OAP metrology mount.[§]

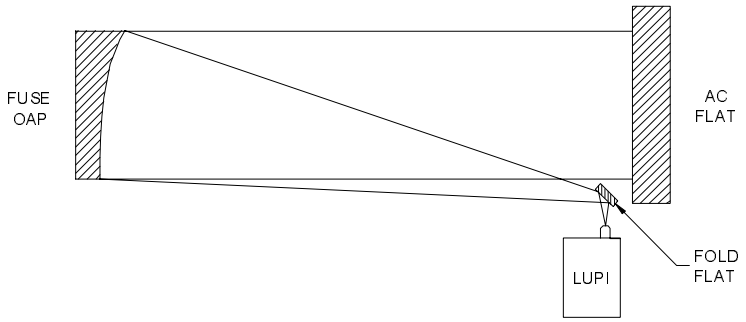

Figure 4. Double-pass figure test setup (top view, not to scale) showing laser unequal path interferometer (LUPI), fold mirror, FUSE OAP, and 21" diameter autocollimation (AC) flat.

Photographs of this setup in the JHU cleanroom are shown in Figure 5. A tent enclosing the setup (except for the LUPI) was erected to control turbulence in the beam path (Section 4). The OAP metrology mount holding a mirror and intermediate plate is shown in Figure 5a. The mount is constructed as a dolly and rides on rails secured to the tabletop. This allowed mirrors and assemblies to be installed clear of the tent framework, then rolled into position inside the enclosure. The tent was originally meant to be a rigid purge enclosure (Section 4.2) and we needed a means to easily transfer mirrors into and out of the enclosure. In the end, the dolly and rail system proved very convenient during mirror loading and unloading, enabling much easier access to the metrology mount.

---

[*] Model MIC-1, Buccini Instrument Co., Wilmington, NC.
[†] Model 02MLE007/028, Melles Griot, Irvine, CA
[‡] Nu-Tek Precision Optical Corporation, Aberdeen, MD, fabricated the AC flat and sling mount.
[§] Nu-Tek also designed and fabricated the metrology mount and rail system.

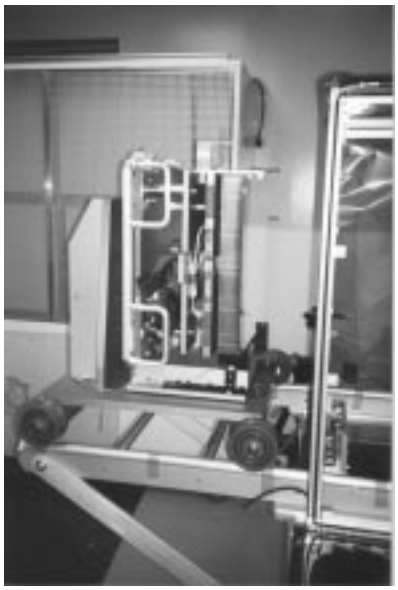

Daniel Carrigan

(a)

Daniel Carrigan

(b)

Figure 5. Implementation of test setup in the cleanroom. (a) Mirror with intermediate plate in the metrology mount. Vertical plate just behind intermediate plate is an adapter mounted to a spare handling plate; used in the absence of a full mirror assembly. Tension spring hanger bar can be seen extending from top of adapter plate; spring itself is not visible. (b) Optical table with autocollimating flat at right end, interferometer on small elevated platform near center, and OAP mirror compartment at left end. Fold flat is mounted on massive black post just inside tent; this was an early source of much vibration. N_2 purge lines can be seen descending from the ceiling.

The video output from the LUPI CCD camera was fed to a PC-based frame grabber supported by fringe analysis software. We used the WYKO Corporation's WISP II software (an old product designed for static fringe analysis) to digitize the fringe pattern, perform the analysis, and produce an optical path difference (OPD) map of the mirror surface. In general, we analyzed six to twelve individual interferograms for a figure test, depending on the time constraints for the test and the desired quality of results. An equal number of interferograms with horizontal and vertical fringes were analyzed, then averaged to produce a final OPD map.

3.2. Coarse Alignment Method

The large number of figure tests we performed required a stable, fixed metrology setup. Placement of the optical components on the table was done only once, with a fair amount of trial-and-error. We preserved the setup afterward by keeping the LUPI position fixed (it could be removed from the table and repeatably reinstalled); this tied the OAP focal point to a fixed position in the setup and preserved the geometry. Small adjustments were made to the LUPI position in the final stages of alignment, but all translation adjustments were reset to their initial positions for the next figure test. With the mirror installed on the metrology mount, supports and/or tension spring adjusted as required, and the mount rolled into the test enclosure, we proceeded with coarse alignment.

Coarse alignment involved judging the fringe pattern on the basis of its qualitative appearance and, using this visual feedback, bringing the system into reasonable alignment (< 1 arcmin). The end result was often far from coarse; the better the inherent figure of the mirror under test, the better we could align the system using this visual method. Although effective for aligning the FUSE mirrors with figure error from 0.025λ to 0.050λ RMS (the worst figure we encountered was 0.10λ), it may not be as straightforward in the presence of large amounts of surface error obscuring the characteristic effects of misalignment in the fringe pattern.

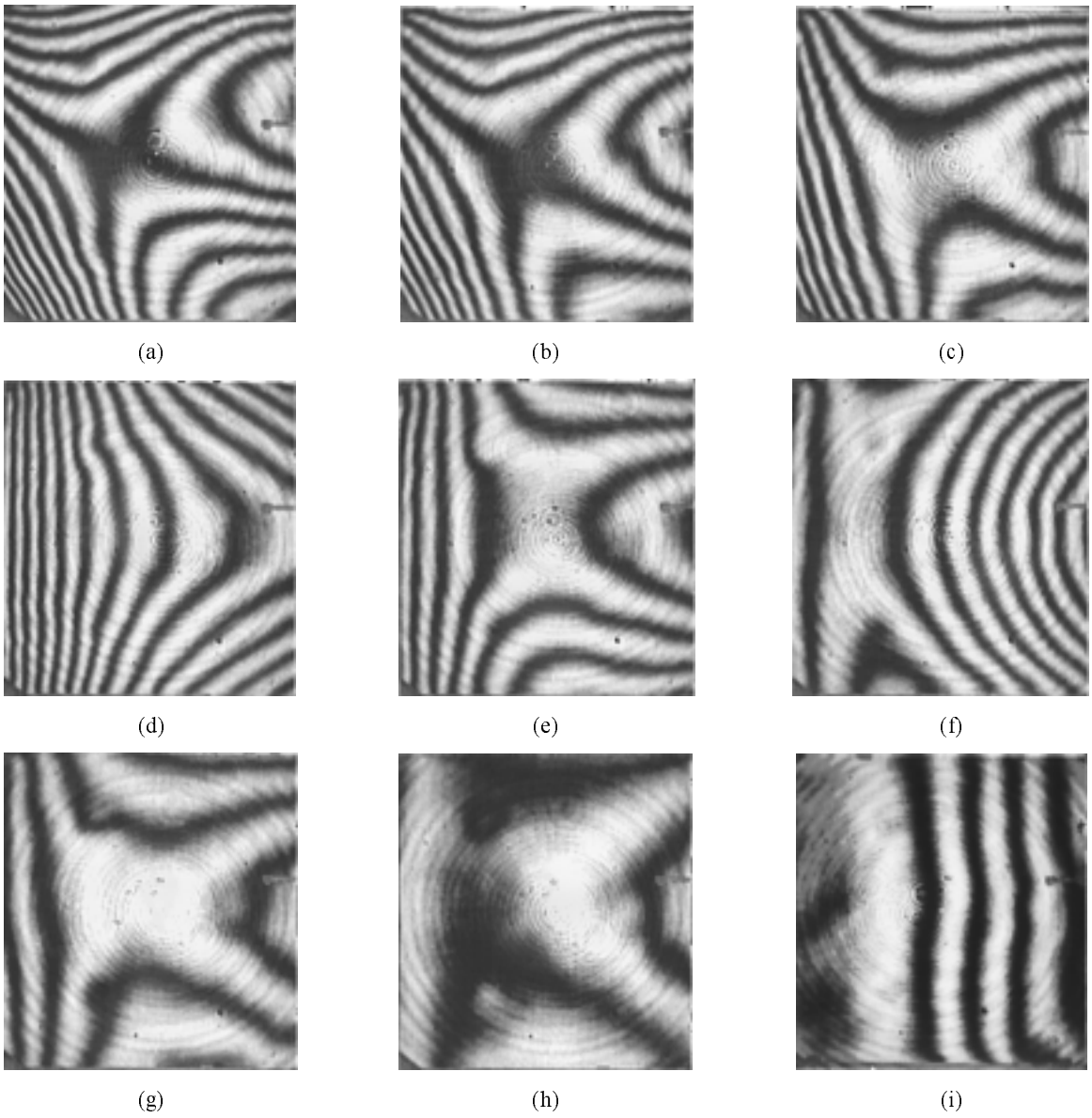

Figure 6. FUSE mirror interferograms depicting the coarse alignment process. (a) Initial alignment containing both horizontal and vertical error. (b) and (c) Progressive vertical alignment. Note the decreasing "rotation" in the fringe pattern. (d) – (f) Good vertical alignment. The left and right interferograms show either side of null. Note the bilateral symmetry in the fringe pattern about a horizontal centerline. (g) and (h) Progressive horizontal alignment. (i) Final visual alignment is judged with tilt fringes added to make residual error (horizontal error is present here) easier to see.

In the detailed procedure given below, two types or directions of misalignment error are discussed, horizontal and vertical. In our case, the OAP was oriented with its vertex to the side, so a line from the center of the OAP through the vertex would be horizontal. Horizontal misalignment results when the LUPI is displaced left or right from the optical axis of the OAP. Vertical misalignment results when the LUPI is offset above or below the optical axis. The directions would be swapped if the OAP was oriented with its vertex up or down; but the alignment procedure would otherwise remain unchanged. The cause of either type of misalignment is the same – the normal of the AC flat is not parallel with the optical axis of the OAP.

The following is a step-by-step procedure of our method. Note that except for the last step, the fringe pattern is observed at null, i.e., no tilt fringes are added. Having two people speeds the process, but it is possible with only one:

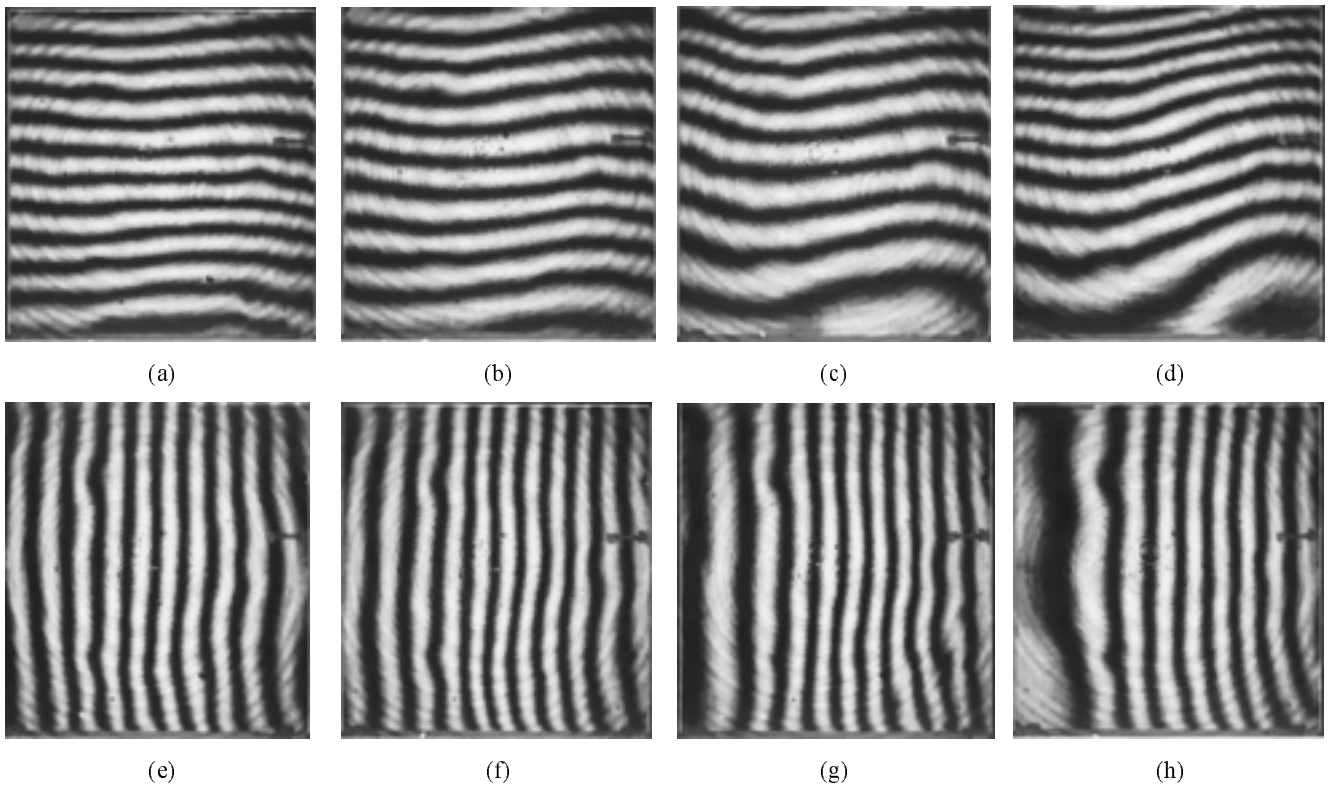

Figure 7. Interferograms from FUSE mirror showing progressive amounts of horizontal misalignment. Note the increasing non-uniformity in the vertical fringe spacing as the horizontal alignment worsens. (a) and (e) Well aligned system. (b) and (f) 30 arcsec of horizontal misalignment. (c) and (g) 60 arcsec of horizontal misalignment. (d) and (h) 120 arcsec of horizontal misalignment.

1. Adjust tip/tilt of the OAP (using metrology mount adjusters) to bring the return beam back into the LUPI and obtain fringes.
2. Focus the LUPI to remove obvious defocus from the fringe pattern. At this point a fringe pattern similar to Figure 6a is typically obtained, containing both horizontal and vertical misalignment.
3. Tip the OAP up or down while following with the AC flat to keep the fringe pattern nulled. Make large motions at first to determine the correct direction to reduce the vertical misalignment. The fringe pattern will "de-rotate" and the number of fringes at null will decrease as vertical error is removed (Figures 6b, c, and e).
4. Continue tipping the OAP and tracking with the AC flat until the obvious vertical error is removed. This is accomplished when a left/right sweep through null produces a strictly horizontal "flow" in the fringe pattern (Figures 6d, e, and f). Note the symmetry in the fringes about a horizontal centerline through the aperture.
5. Switch to tilting the OAP left or right and tracking with the AC flat to find the direction needed to remove the horizontal error. Observe the fringe pattern at null to look for reduction in the number of fringes present (Figures 6e, g, and h).
6. Once a good null pattern is obtained (i.e., when it becomes hard to tell what to do next), add a few vertical tilt fringes (usually done by tilting the LUPI's reference flat) to look for residual errors of both types. Horizontal error will show up as a non-uniform spacing in the fringes (Figure 6i and 7), while vertical error will manifest itself in a fanning of the fringes from top to bottom (Figure 8).
7. Tweak the alignment to remove all visible signs of either error. Refer to Figures 7 and 8 to see how the two errors are manifested in the presence of tilt fringes. Use whichever two optical components have the most precise motion adjustments (the LUPI and AC flat, in our case).

At this point, the system is aligned to the limit of visually discerning changes in the fringe pattern. We could usually complete this procedure within a half-hour, and to within 15 arcsec with a low (0.025λ RMS) surface error mirror.

3.3. Fine Alignment Method

After visual alignment, we switched to computer analysis of the interferograms for further refinement. It should be noted that when testing mirrors with low figure error (0.025–0.030λ RMS), fine alignment was often just confirmation that the visual procedure had found the optimum alignment to the limit of our system. In general, fine alignment proceeded as follows:

1. Analyze three interferograms and record RMS OPD errors. Also take note of the general character of the OPD map, noting the effect of any obvious vertical or horizontal misalignment (e.g. a high corner or edge).
2. Step the LUPI vertically by a set amount (usually 15 arcsec in our case), and record position. We typically started with vertical steps because it was easy to spot vertical error in the OPD plots.
3. Tip the AC flat to reacquire the fringe pattern.
4. Analyze three interferograms, record RMS OPD errors for this position, and look for changes in the OPD map indicative of obvious misalignment.
5. Continue stepping vertically with the LUPI, tipping the AC flat, and analyzing interferograms until the RMS errors begin to clearly get worse. The OPD map will show obvious signs of vertical error (corners on vertex edge curling up/down).
6. If a vertical alignment with minimum RMS OPD error can be determined, proceed to horizontal fine alignment (step 7); otherwise return to the starting point and begin stepping in the opposite direction until a minimum in RMS error can be determined.
7. Set the interferometer to the position of minimum RMS error and tip the AC flat to reacquire the fringe pattern.
8. Repeat the above procedure, stepping the LUPI horizontally and tilting the AC flat, until a minimum in RMS error can be similarly determined.

This procedure could typically be accomplished with several (~ five) steps in each direction, if the step size was appropriately matched to the amount of figure error present. This could usually be judged from coarse alignment based on the final fringe pattern and the magnitude of adjustment required to see a definitive worsening/improvement in the fringes. Fine alignment usually took 30 to 60 minutes to complete, depending on environmental conditions.

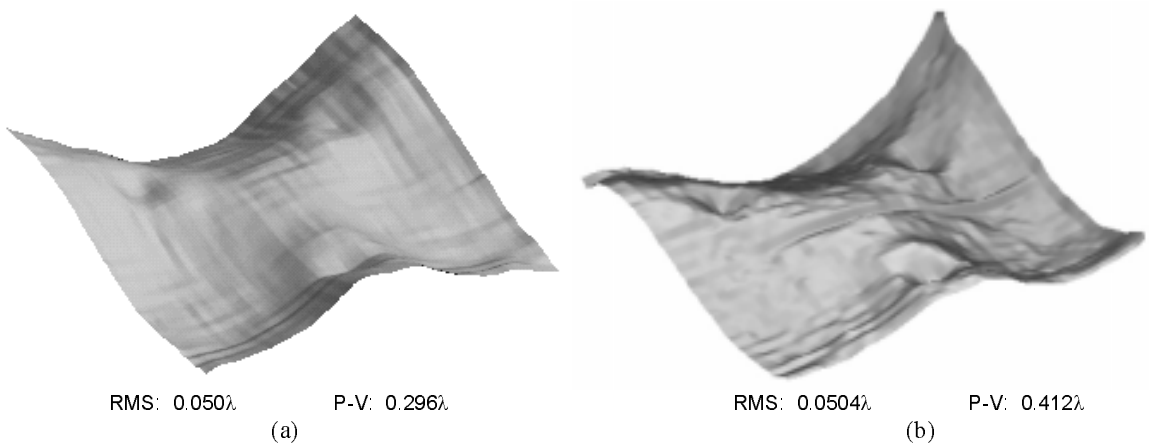

Figure 9. Surface plots of optical path difference (OPD) files from figure tests of the flight spare mirror. Vertex is toward the front in this view. (a) JHU test with Buccini MIC-1 interferometer (average of 10 single-interferogram OPD maps). (b) Tinsley test with Phase Shift Technology Mini-Fiz interferometer (smoothed average of many individual phase-shifting runs). Note that the JHU test had the mirror supported on the right edge as shown in the plots, whereas the Tinsley test had the mirror supported vertex up. The three "craters" are flexure bond locations, caused by stress in the epoxy bondline.

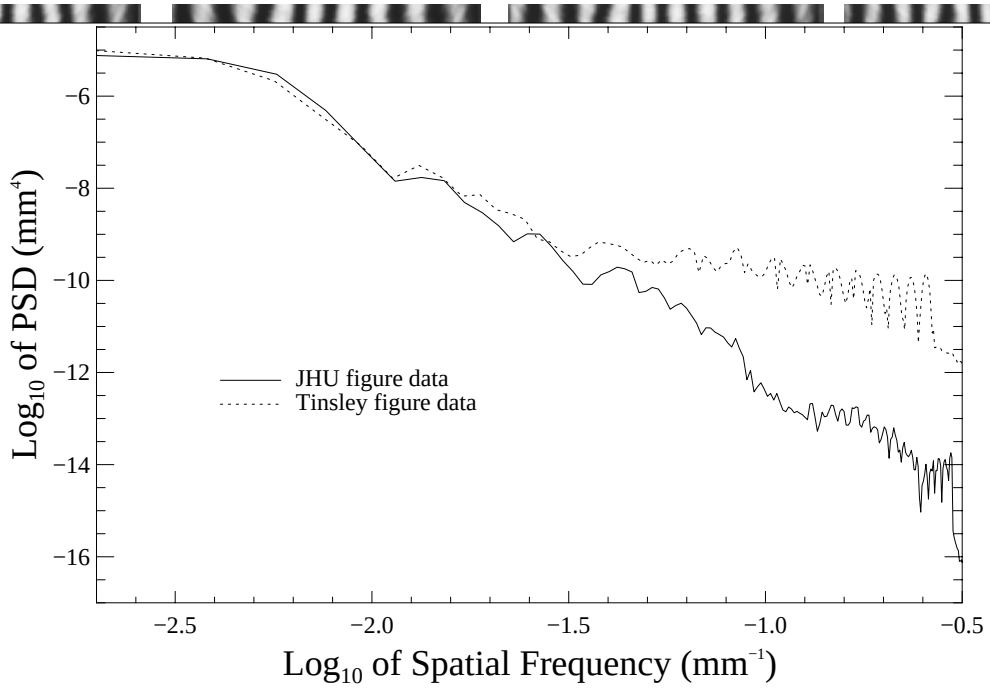

Figure 10. 2-D power spectral density (PSD) from figure tests of the flight spare mirror at JHU and Tinsley. The first four Zernike terms (piston, tilts, and focus) were removed from each OPD map before generating the PSD. The falloff in the JHU data at higher spatial frequencies is evident, indicative of reduced frequency response in the JHU figure test at smaller spatial scales.

3.5. Other Alignment Methods

We initially considered using a phase-shifting interferometer in conjunction with a software fitting routine for aligning the FUSE flight mirrors. This scheme would have provided OPD surface maps with much greater spatial sensitivity (Section 3.4 and Figures 9 and 10). We decided against such a system for several reasons: After delivery of the mirrors from Tinsley, we were primarily concerned with detecting large-scale figure error induced by the remainder of the assembly process, so high-spatial sensitivity was unnecessary, especially given the additional cost of a phase-shifting interferometer. Furthermore, the extreme test conditions vis-à-vis vibration and turbulence associated with the cleanroom environment probably would have made testing impracticable (Section 4). The simpler and less expensive LUPI and static interferogram analysis presented here is a more robust approach in light of these environmental challenges and the necessary flexibility of our test program. A software routine still could have been used for alignment optimization, but the "feedback loop" would have been slow given the time it took to us produce a single, high quality, averaged OPD map. We found the visual interpretation of fringe patterns to be an efficient and intuitive procedure.

Bond and Pipan[9] present a method for coarse alignment of OAPs via analysis of the image of the spot produced by the return beam from a double-pass setup. This procedure would have required the ability to switch the focus of the LUPI output leg from a focal point for viewing the return spot to the OAP aperture for fringe analysis, and perhaps between detectors (human eye vs. LUPI CCD camera). This reconfiguring would have probably lengthened the alignment process, and our ability to quickly align the mirrors proved critical later in the mirror program when attempting to overcome environmental challenges (Section 4.2). We did not try this method.

Other OAP alignment methods were considered.[10] However, the aforementioned methods and the technique we applied would yield the fine alignment necessary for figure testing the FUSE mirrors. They also present more straightforward techniques given our various mounting conditions and constraints.

4. ENVIRONMENTAL CHALLENGES

4.1. Cleanroom Air Flow and Vibration

Figure testing in the cleanroom at JHU presented challenging vibration and turbulence problems. A Llumalloy tent enclosure used for the SiC mirrors, which did not require purge during testing, eliminated turbulence problems directly associated with the cleanroom air flow, helped thermally stabilize the setup (the warm laser source for the LUPI was housed outside the tent), and helped maintain the environment in the immediate vicinity of the mirror at class 1000 cleanroom standards.

However, vibration induced by the cleanroom air flow still presented a problem when trying to acquire stable fringes for fine alignment and figure testing. The vibration upset the fringe pattern such that it typically took ~20 attempts with the frame grabber to acquire an interferogram without severe video interlacing vibration artifacts. The magnitude of this vibration was about < ½ arcsec (a few fringes) in amplitude of boresight error for a range of frequencies easily observable with the video output and un-aided eye. Thus, figure testing was possible, but time-consuming when contending with the cleanroom airflow.

We essentially fully mitigated these severe vibration problems by testing with the cleanroom blowers off. If the test duration was kept under a few hours, this did not pose a contamination hazard. The optical setup still experienced mechanical vibration associated with the building air handling units, etc., in spite of using a vibration-dampening optical table. The amplitude of this residual vibration was about < 0.1 arcsec (1 fringe) for the same range of observable frequencies. However, without the continuous air flow around the tent and warm LUPI, the setup required about an hour to thermally stabilize upon shutoff of the air handler prior to testing. This method was therefore about as time-consuming in the end as testing with the blowers on, but less operator-intensive. In hindsight, we probably should have added substantial mass to our optical mounts to make them less susceptible to vibration.

4.2. Sensitivity to Moisture

As mentioned previously, the far-UV reflectivity of the LiF-coated mirrors is sensitive to exposure to atmospheric water vapor. Based on data from previous programs,[5,11] we developed a budget for exposure to typical laboratory ambient conditions (e.g. 25°C, 50% R/H) throughout mirror subsystem assembly and test and instrument-level integration: the total exposure of the LiF coatings to a non-purged environment was to be less than 100 hours. We expected a corresponding reflectivity degradation of about 20%. We therefore carried out mirror assembly with the optical surface of each mirror protected and under constant N_2 purge.

We constructed a purge enclosure around the optical setup (not shown). The walls were made from 0.375" polycarbonate sheets bolted to an extruded aluminum frame, which itself was attached to the optical table. The table surface was covered with a sheet of Llumalloy to seal the pattern of tapped holes. The purge box was sealed with Viton rubber tubing. We used a pneumatically controlled door to divide the purge box into two sections, one containing the bulk of the optical path and one for the flight mirror under test. This allowed us to load and unload flight mirrors without losing the bulk of the N_2 purge to the cleanroom. Alignment controls on the autocollimating flat and metrology mount were accessed via glove ports in the walls of the enclosure. The LUPI test beam entered and exited the enclosure through a small hole in one of the side panels.

Unfortunately, we found that this rigid polycarbonate enclosure amplified the already severe vibrations to such a degree that figure testing was impossible with the cleanroom blowers on. With the blowers off, vibration was about the same as in the Llumalloy tent with the blowers on. However, stratification problems inside the enclosure plagued our attempts at testing with the polycarbonate enclosure – problems we had not encountered with the tent. At this point, the schedule was getting very tight and we needed a reliable way to figure test the mirror assemblies before delivery to the instrument team. We therefore abandoned the polycarbonate box in favor of a simple, non-purged tent (same aluminum frame with Llumalloy and polyethylene walls; Figure 5b) designed to help minimize turbulence along the optical path while running the cleanroom blowers and maintaining thermal stability. This setup with thin, flexible walls imparted no additional vibration to the optical bench, but was not sealed enough to purge out the water vapor. We relied on quickly mounting and aligning the flight mirrors to minimize the exposure of the LiF mirrors to non-purged conditions. Except for the final figure test, LiF mirror testing became quick checks to insure acceptable surface error. Our ability to quickly mount, align, and test a flight mirror using the methods described in Section 3 proved of great importance in minimizing exposure of the sensitive optics.

Toward the end of the mirror program, we were able to successfully figure test the flight spare mirror under purge using the tent enclosure with Llumalloy walls sealed with Kapton tape. This was part of the image test performed at 184.9 nm on the flight spare mirror.[4] Note that the spare mirror was coated with SiC, so the purged environment was not as critical for this optic from the standpoint of preserving UV reflectivity. Turbulence was a significant problem while actively injecting N_2 into the tent enclosure, but we found we could shut off the purge for > 10 minute periods and align and figure test in a sufficiently stable environment. We did not have time to experiment with other purge gases (such as helium) which may have provided a better test environment.

5. CONCLUSION

We were able to rapidly align and figure test off-axis parabolic mirrors for a far-UV astronomy instrument under challenging cleanroom conditions. The test environment posed many obstacles that were overcome as much by trial-and-error as careful planning. We have presented a general technique for interferometric alignment of OAPs using only the hardware and software already needed for the figure test. This technique was efficient for testing OAPs with low inherent figure error ($< 0.050\lambda$ RMS).

ACKNOWLEDGMENTS

FUSE is supported through the NASA Explorers Program office at Goddard Space Flight Center (GSFC), and managed within the Center for Astrophysical Sciences at JHU (NASA contract NAS5-32985). The authors gratefully acknowledge: Dr. Timo T. Saha of NASA/GSFC for generating the PSD curves shown in Figure 10; Daniel Carrigan, formerly of Swales and Associates, Inc., for his patience and precision; Daniel Vukobratovich of National Optical Astronomy Observatories for

his advice; Dr. James C. Wyant of the Optical Sciences Center, University of Arizona, formerly of the WYKO Corp., for assistance with fringe analysis software; and Nu-Tek Precision Optical Corp., Aberdeen, Md., for advice and assistance.

REFERENCES

1. E. Wilkinson, J. C. Green, S. N. Osterman, K. R. Brownsberger, and D. J. Sahnow, "Integration, alignment, and initial performance results of the Far Ultraviolet Spectroscopic Explorer (FUSE) spectrograph," *Proc. SPIE* **3356**, pp. 18-29, 1998.
2. M. J. Kennedy, S. D. Friedman, R. H. Barkhouser, J. Hampton, and P. Nikulla, "Design of the Far Ultraviolet Spectroscopic Explorer mirror assemblies," *Proc. SPIE* **2807**, pp. 172-183, 1996.
3. R. G. Ohl, R. H. Barkhouser, M. J. Kennedy, and S. D. Friedman, " Assembly and test-induced distortions of the FUSE mirrors – lessons learned," *Proc. SPIE* **3356**, pp. 854-865, 1998.
4. R. G. Ohl, S. D. Friedman, T. T. Saha, R. H. Barkhouser, and H. W. Moos, "Optical testing of the Far Ultraviolet Spectroscopic Explorer primary mirrors and predicted on-orbit performance," *Proc. SPIE* **3782**, 1999.
5. J. F. Osantowski, R. A. M. Keski-Kuha, H. Herzig, A. R. Toft, J. S. Gum, and C. M. Fleetwood, "Optical Coating Technology for the EUV," *Adv. Space Res.* **11**, pp. 185-201, 1991.
6. T. T. Saha, D. B. Leviton, and P. Glenn, "Performance of ion-figured silicon carbide SUMER telescope mirror in the vacuum ultraviolet," *Appl. Opt.* **35**, pp. 1742-1750, 1996.
7. J. E. Harvey, *Final Report for FUSE Telescope Performance Predictions*, Consulting Agreement under NASA Contract NAS5-32985 (Johns Hopkins University, Baltimore, Md., 1996).
8. J. B. Houston, C. J. Buccini, and P. K. O'Neill, "A laser unequal path interferometer for the optical shop," *Appl. Opt.* **6**, pp. 1237-1242, 1967.
9. C. Bond and C. A. Pipan, "How to align an off-axis parabolic mirror," *Proc. SPIE* **1113**, pp. 236-248, 1989.
10. M. C. Ruda, *Understanding Optical Alignment Techniques*, course notes from College of Engineering, University of Wisconsin-Madison, 1995.
11. J. Gum, NASA/Goddard Space Flight Center, personal communication